Epidemic dynamics of two species of interacting particles on scale-free networks

Yong-Yeol Ahn and Hawoong Jeong
Department of Physics, Korea Advanced Institute of Science and Technology, Daejeon 305-701, Korea

Naoki Masuda
Amari Research Unit, RIKEN Brain Science Institute, 2-1, Hirosawa, Wako, Saitama 351-0198, Japan

Jae Dong Noh
Department of Physics, University of Seoul, Seoul 130-743, Korea

(Received 31 August 2006; revised manuscript received 9 October 2006; published 21 December 2006)

We study the nonequilibrium phase transition in a model for epidemic spreading on scale-free networks. The model consists of two particle species A and B, and the coupling between them is taken to be asymmetric; A induces B while B suppresses A. This model describes the spreading of an epidemic on networks equipped with a reactive immune system. We present analytic results on the phase diagram and the critical behavior, which depends on the degree exponent γ of the underlying scale-free networks. Numerical simulation results that support the analytic results are also presented.

DOI: 10.1103/PhysRevE.74.066113 PACS number(s): 89.75.Hc, 05.70.Ln, 87.19.Xx

Network concept has been emerging as a useful tool for the study of complex interconnected systems [1–3]. It allows us to study structure and dynamics of those systems in various disciplines in a simple unified manner. Many networks in nature share an intriguing property of the power-law degree distribution $P(k) \sim k^{-\gamma}$ with the degree exponent γ, where $P(k)$ is the probability of a node having k links. A network with this property is called a scale-free (SF) network [1], examples of which include the world-wide web [4], the Internet [5], and the human sexual contact network [6], and so on.

The broad degree distribution of the SF network brings about various interesting phenomena. Particularly we are interested in epidemic spreading. Networked systems are susceptible to epidemics, which may be computer viruses in computer networks or infectious diseases in social contact networks of individuals. Robustness against the epidemic spreading is one of the key elements for a proper function of networks. Researchers have studied the characteristic feature of the epidemic spreading in the SF network and the efficient immunization strategy suitable for the SF network [7–12].

There are hubs with a large number of links in the SF network. This structure makes it vulnerable to an epidemic since it can spread easily through those hubs. It is found that an epidemic even with an extremely small spreading rate never ceases spreading in the SF networks with $\gamma \leqslant 3$ [7,8]. In those networks, the random immunization where all nodes are immunized or vaccinated with an equal but finite probability becomes inefficient. Instead, the targeted immunization where hubs are immunized preferentially proves to be efficient [9–11].

In the study of the epidemic spreading, one usually considers the dynamics of malicious agents on bare or immunized networks. On the other hand, the following examples show that the competing spreading dynamics between malicious agents and immunizing agents are also important. Recently, the worm "Code Red" almost paralyzed the whole Internet by flooding it with lots of useless packets [13]. After the outbreak, there appeared the so-called worm-killer worm "Code Green" which was meant to seek out and kill the malicious worm [14]. Although it also flooded the network and did more harm than good, it hinted a possibility of contagious vaccination. The competing dynamics is also observed inside living organisms. When pathogens invade and spread, immune cells are stimulated. The awaken immune cells then replicate themselves and get rid of the pathogens [15]. The phenomenon of *cross immunity* between competing pathogens is another example [12]. If populations are exposed to a certain disease, then they become immune to the other for certain pairs of diseases, e.g., Hansen's disease and tuberculosis [16].

In this work, we introduce a model that mimics the competing spreading dynamics and study the phase transition it displays on SF networks. The model consists of two species (A and B) particles, one of which infects nodes and the other of which heals the infection. They may represent worms (A) and worm-killer worms (B) in computer networks or malicious pathogens (A) and immune cells (B) in living organisms.

At each time step particles evolve according to the following dynamic rule: An A particle either annihilates spontaneously with the probability p_A, or creates a particle at each neighboring node with the probability $q_A = 1 - p_A$. The fraction $1-\lambda$ (λ) of the created particles are of species A (B). A B particle either annihilates spontaneously with the probability p_B, or creates another B particle at one of the neighboring nodes selected randomly with the probability $q_B = 1 - p_B$. The creation attempt is rejected if a target node is already occupied by the same species particle. When two particles of different species become to occupy the same node, the A particle is removed with the probability μ.

Each node may be empty, occupied by a particle A, or occupied by a particle B. Such a node can be interpreted as a healthy or susceptible, infected, or immunized individual, respectively. Then the process with p_A and $q_A(1-\lambda)$ corresponds to spontaneous healing and infection, respectively.

The process with $q_A\lambda$ corresponds to activation of an immune system. The spontaneous annihilation of B particles takes account of the fact that immunization may not be permanent. The parameter μ describes the efficiency of the immune system in healing the infection.

Note that the particles A and B have different branching rules. A particle A branches offsprings to *all* neighboring nodes as in the susceptible-infected-susceptible (SIS) model [7], while a particle B branches an offspring to *one* of the neighboring nodes as in the contact process (CP) [17]. This difference can be negligible in networks with the narrow degree distribution, but it makes a big difference in SF networks [17]. We adopt the less-reproductive CP dynamics for the particle B since it would be costly to activate an immune system in real systems. The model was studied in networks with a narrow degree distribution [18]. As we will see, the model shows much richer properties in SF networks.

The model displays three stationary state phases denoted by (0,0), $(0,B)$, and (A,B). They are distinguished with the stationary state density of each particle species. Both species are *inactive* with zero density in the (0, 0) phase. In the $(0,B)$ phase, the A particles are inactive while the B particles are *active* with a nonzero density. Both species are active with nonzero densities in the (A,B) phase. Due to the asymmetric nature of the interaction, one does not have a phase in which the A particles are active and the B particles are inactive. All nodes are healthy in the (0, 0) and $(0,B)$ phases. The healthy state requires that the B particles are active in the $(0,B)$ phase, which is not the case in the (0, 0) phase. In this sense, the $(0,0)$ phase is the ideal one since the remnant B particles would cost system resources.

We will study the phase transitions and the critical behaviors in SF networks by adopting the rate equation approach which proves useful for a single species or multispecies particle systems [7,19]. It is assumed that the particle density at a node is given by a function of its degree only. Let a_k and b_k be the density of A and B particles on nodes with degree k, respectively. Then, it is straightforward to show that they satisfy the coupled rate equations

$$\dot{a}_k = -p_A a_k + q_A(1-\lambda)k(1-a_k)\Theta_A(k) - \mu k a_k \Theta_B(k),$$
$$\dot{b}_k = -p_B b_k + q_B k(1-b_k)\Theta_B(k) + q_A \lambda k(1-b_k)\Theta_A(k), \tag{1}$$

where $\Theta_A(k)$ $[\Theta_B(k)]$ denotes the probability that a node with degree k is infected by a particle A (B) from each of its neighboring nodes. They are given by $\Theta_A(k) = \Sigma_{k'} a_{k'} P(k'|k)$ and $\Theta_B(k) = \Sigma_{k'} b_{k'} P(k'|k)/k'$, respectively. Here $P(k'|k)$ is the conditional probability that a node at one end of a link have the degree k' under the condition that the other end of the link has the degree k. The different form of Θ_A and Θ_B is due to the different spreading dynamics of the two particle species. The conditional probability can take care of a degree correlation [20]. In this work, we only consider networks with no degree correlation, that is, $P(k'|k) = k'P(k')/\langle k\rangle$ with the degree distribution $P(k) \sim k^{-\gamma}$ and the mean degree $\langle k\rangle$ [20]. Then, one obtains that

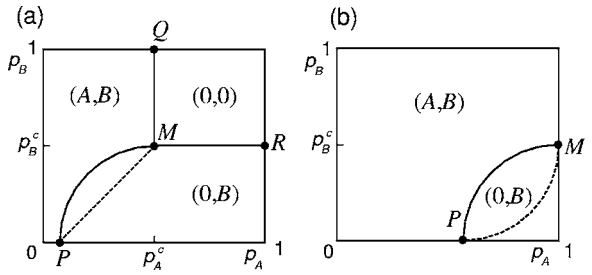

FIG. 1. The schematic phase diagram in SF networks with $\gamma > 3$ in (a) and $\gamma \leqslant 3$ in (b). The phase boundary $\overline{MP}$ changes its shape as γ varies. In (a), it is tangential to $\overline{MR}$ for $\gamma < 4$ (solid line) and nontangential to $\overline{MR}$ or $\overline{MQ}$ for $\gamma \geqslant 4$ (dashed line). In (b), it is parallel to p_A axis at M for $\gamma > 5/2$ (solid line), and to p_B axis near M for $\gamma < 5/2$ (dashed line).

$$\Theta_A = \frac{1}{\langle k\rangle}\sum_k k a_k P(k), \quad \Theta_B = \frac{1}{\langle k\rangle}\sum_k b_k P(k). \tag{2}$$

They are related to the particle density and will be used as the order parameter.

In the stationary state ($\dot{a}_k = \dot{b}_k = 0$), the order parameter satisfies the coupled self-consistency equations

$$\Theta_A = f(\Theta_A, \Theta_B) \equiv \frac{1}{\langle k\rangle}\sum_k \frac{\tilde{q}_A \Theta_A k^2 P(k)}{1 + (\tilde{q}_A \Theta_A + \tilde{\mu}\Theta_B)k}, \tag{3a}$$

$$\Theta_B = g(\Theta_A, \Theta_B) \equiv \frac{1}{\langle k\rangle}\sum_k \frac{(\tilde{\lambda}\Theta_A + \tilde{q}_B \Theta_B)k P(k)}{1 + (\tilde{\lambda}\Theta_A + \tilde{q}_B \Theta_B)k}, \tag{3b}$$

where $\tilde{q}_A \equiv \frac{q_A}{p_A}(1-\lambda)$, $\tilde{\mu} \equiv \frac{\mu}{p_A}$, $\tilde{\lambda} \equiv \frac{q_A}{p_B}\lambda$, and $\tilde{q}_B \equiv \frac{q_B}{p_B}$. Note that, without the interaction ($\tilde{\lambda} = \tilde{\mu} = 0$), the self-consistency equations are decoupled, each of which has been studied separately [9,17].

The self-consistency equations allow us to determine the phase diagram, whose schematic plot is shown in Fig. 1. Let us summarize the result first: For $\gamma > 3$ [Fig. 1(a)], we find that the system exhibits the three phases (0, 0), $(0,B)$, and (A,B). Across the line $\overline{MR}$, A particles remain inactive and B particles become active. Across the line $\overline{QM}$, both particles become active simultaneously. Across the line $\overline{MP}$, B particles are already active and the A particles become active. The three phase transition lines merge into the multicritical point M.

On the other hand, the system exhibits the only two phases $(0,B)$ and (A,B) for $\gamma \leqslant 3$ [Fig. 1(b)]. Without the B species, the A species would always be in the active phase for $\gamma \leqslant 3$ [7]. The existence of the phase $(0,B)$ implies that one can prevent an epidemic from spreading even in the SF networks with $\gamma \leqslant 3$. The nonexistence of the phase (0, 0), however, implies that the immunization is possible only when the species B is kept to be in the active state, which may cost system resources.

Now we sketch briefly the way the phase diagram is obtained, details of which will be presented elsewhere [21]. It is obvious that $\Theta_A = \Theta_B = 0$ is a solution of the self-consistency equation. One can obtain the boundary of the phase (0, 0)

from the condition for the existence of nonzero solutions for Θ_A or Θ_B. From Eq. (3a), we find that $f(0,0)=0$ and $f(\Theta_A,0)\leqslant 1$ and $\partial^2 f(\Theta_A,0)/\partial\Theta_A^2<0$ for all Θ_A. So a nonzero solution for Θ_A exists when $\partial f(0,0)/\partial\Theta_A=\tilde{q}_A\langle k^2\rangle/\langle k\rangle\geqslant 1$ with $\langle k^2\rangle$ the second moment of the degree. This gives the phase boundary $\overline{QM}$ at $\tilde{q}_A=\langle k\rangle/\langle k^2\rangle$ or at $p_A=p_A^c$ with

$$p_A^c=\frac{(1-\lambda)\langle k^2\rangle/\langle k\rangle}{1+(1-\lambda)\langle k^2\rangle/\langle k\rangle}. \tag{4}$$

Similarly, a nonzero solution for Θ_B exists when $\partial g(0,0)/\partial\Theta_B=\tilde{q}_B\geqslant 1$, which gives the phase boundary $\overline{MR}$ at $\tilde{q}_B=1$ or at $p_B=p_B^c=1/2$. For $\gamma\leqslant 3$, $\langle k^2\rangle$ is infinite, $p_A^c=1$, and the phase (0, 0) vanishes.

At the phase boundary $\overline{MP}$, $\Theta_A=0$ and Θ_B has a nonzero value Θ_B^* satisfying $\Theta_B^*=g(0,\Theta_B^*)$. We also have that $\partial f(0,\Theta_B^*)/\partial\Theta_A=1$ since Θ_A begins to deviate from zero at that line. These two equations define the phase boundary $\overline{MP}$. Near the point M, the phase boundary is given by

$$\epsilon_B\sim\begin{cases}\epsilon_A^{1/\min(1,\gamma-3)}, & \gamma>3,\\ \epsilon_A^{(\gamma-2)/(3-\gamma)}, & \gamma<3,\end{cases} \tag{5}$$

for small $\epsilon_A=p_A^c-p_A$ and $\epsilon_B=p_B^c-p_B$ [21].

We also studied the critical behavior of the order parameter near the phase transitions by analyzing the property of the functions f and g at small values of Θ_A and Θ_B. We found that the order parameter shows the power-law scaling

$$\Theta_{A,B}\sim\epsilon^{\beta_{A,B}} \tag{6}$$

with the γ dependent critical exponents β_A and β_B for $\gamma\neq 3$. The critical exponents have different values at different critical lines. The results are summarized in Table I. The model displays interesting multicritical behaviors at the multicritical point M, which will be discussed elsewhere [21].

It is noteworthy that the model displays the peculiar critical behaviors at $\gamma=3$. Let us take the degree distribution as $P(k)=ck^{-3}$ for $k_0\leqslant k$ with a normalization constant c and a degree cutoff k_0. With the continuum k approximation in Eq. (3), the functions f and g are given by $f=\frac{c\tilde{q}_A\Theta_A}{\langle k\rangle}\ln\left(\frac{1+k_0X}{k_0X}\right)$ and $g=Y-\frac{c}{\langle k\rangle}Y^2\ln\left(\frac{1+k_0Y}{k_0Y}\right)$ with $X\equiv\tilde{q}_A\Theta_A+\tilde{\mu}\Theta_B$ and $Y\equiv\tilde{\lambda}\Theta_A+\tilde{q}_B\Theta_B$. The logarithmic dependence leads to the following peculiar behaviors [21]: Let $\epsilon_A=1-p_A$ and $\epsilon_B=1/2-p_B$ be the deviation from M at $p_A=1$ and $p_B=1/2$. The phase boundary $\overline{MP}$ is given by

TABLE I. The exponents β_A and β_B associated with each phase transition line. For $\gamma\leqslant 3$, the phase (0,0) denotes the line with $p_A=1$ and $p_B>p_B^c$.

		$(0,0)\rightarrow(A,B)$	$(0,0)\rightarrow(0,B)$	$(0,B)\rightarrow(A,B)$
$\gamma>4$	β_A	1		1
	β_B	1	1	
$3<\gamma<4$	β_A	$\frac{1}{\gamma-3}$		1
	β_B	$\frac{1}{\gamma-3}$	1	
$2<\gamma<3$	β_A	$\frac{\gamma-2}{3-\gamma}$		1
	β_B	$\frac{1}{3-\gamma}$	$\frac{1}{\gamma-2}$	
$\gamma=3$	Θ_A	$\sim e^{-d/\epsilon_A}/\epsilon_A$		1
	Θ_B	$\sim e^{-d/\epsilon_A}$	1	

$$\epsilon_B\sim\frac{1}{\epsilon_A}e^{-d/\epsilon_A} \tag{7}$$

with a constant d for small ϵ_A and ϵ_B. When one approaches M from the phase (A,B), the order parameter exhibits a path dependent critical behavior. Along the path with $\epsilon_B=0$ that is tangential to $\overline{MP}$, we find that

$$\Theta_A\sim\frac{1}{\epsilon_A^2}e^{-2d/\epsilon_A},\quad \Theta_B\sim e^{-d/\epsilon_A}. \tag{8}$$

Along nontangential paths with finite $\epsilon_A/|\epsilon_B|$, we find that

$$\Theta_A\sim\Theta_B\sim e^{-d/\epsilon_A}. \tag{9}$$

In contrast to the power-law scaling at $\gamma\neq 3$, the order parameter as well as the phase boundary has the essential singularity at $\gamma=3$. The order parameter also has the essential

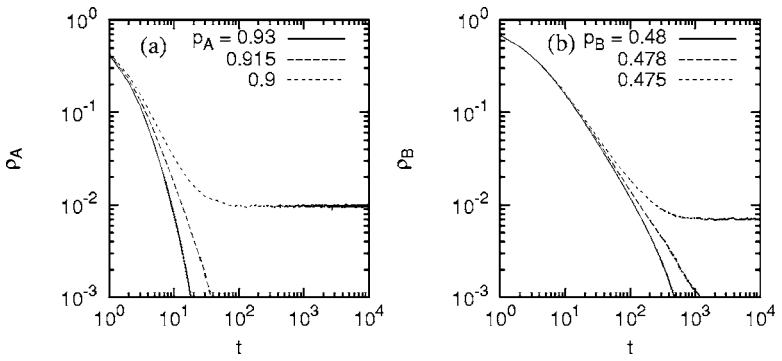

FIG. 2. Density decay at $\gamma=3.5$. In (a) ρ_A is plotted at $p_B=0.9$, and in (b) ρ_B is plotted at $p_A=0.99$.

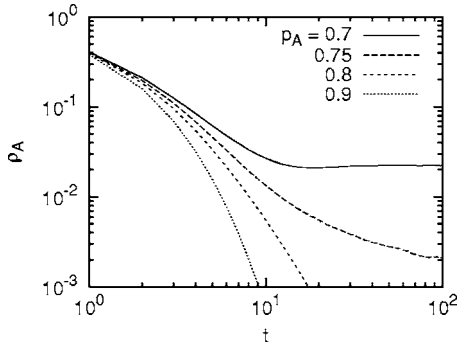

FIG. 3. Density decay on SF networks with $\gamma=2.75$. ρ_A is plotted for several values of p_A with $p_B=0.3$.

singularity near the line with $p_A=1$ and $p_B>p_B^c$ (see Table I). That is, the transition is the infinite order transition. The infinite order transition was reported recently in the percolation problem and the equilibrium Ising model on growing networks [22,23].

In order to confirm the phase diagram, we performed numerical simulations on SF networks generated by using the so-called static model [24]. Initially networks are filled with the particles, and the density ρ_A and ρ_B of each particle species is measured and averaged over at least 2000 simulations and 10 network realizations. All simulations were performed with $\lambda=\mu=0.5$. All numerical data presented below were obtained on the static model networks with $N=64\times10^4$ nodes and the mean degree $\langle k\rangle=12$.

We present the numerical data from the SF networks with $\gamma=3.5$ in Figs. 2(a) and 2(b). They show the signature of the phase transition from (0, 0) to (A,B) at $p_A^c\simeq0.915$ and (0, 0) to $(0,B)$ at $p_B^c\simeq0.478$, respectively. These numerical data confirms the existence of the three phases for $\gamma>3$.

At $\gamma=2.75$, we performed the simulations at $p_B=0.3$ and for several values of p_A in order to examine the existence of the $(0,B)$ phase. The numerical data presented in Fig. 3 clearly show that the A species is in the active phase at $p_A=0.7$ and in the inactive phase at $p_A=0.9$. Although it is hard to locate the critical point accurately, the numerical data supports the analytic prediction that the A species can be inactive even for $\gamma\leqslant3$ in our model. At $\gamma=2.75$, we also performed the simulations at $p_B=0.9$ and at several values of p_A close to 1 in order to examine whether the phase (0, 0) exists or not. Numerical data obtained on the networks of sizes up to $N=64\times10^4$ nodes indicate that the A species is in the active phase at least up to $p_A=0.99$ and that the A species become more active as N increases [21]. So we conclude that the phase (0, 0) does not exist in the asymptotic $N\rightarrow\infty$ limit.

In summary, we have studied the two-species epidemic model on SF networks. The two species A and B are coupled asymmetrically in that the former induces the latter whereas the latter suppresses the former. Our model is aimed at describing the spreading dynamics of competing malicious pathogens (A particles) and reactive immunizing agents (B particles) on complex SF networks. The model is shown to have the different phase diagram depending on whether $\gamma>3$ or $\gamma\leqslant3$ (see Fig. 1). Our results show that one can prevent the epidemic from prevailing even in SF networks with $\gamma\leqslant3$. That is, cross immunization [12] and contagious vaccination [13] strategy using competing spreading dynamics can be applied successfully for epidemic control even in very inhomogeneous networks. The results also show that it requires that the immunizing agents should be kept in the active phase for $\gamma\leqslant3$, which is not necessary for $\gamma>3$. We have also investigated the critical behaviors associated with the phase transitions. Especially, when $\gamma=3$, the phase transitions are infinite order transitions with the essential singularity in the order parameters.

This work was supported by Korea Research Foundation Grant No. KRF-2004-041-C00139. Two of the authors (Y.Y.A. and H.J.) were supported by the Ministry of Science and Technology through Korean Systems Biology Research Grant No. M10309020000-03B5002-00000. One of the authors (N.M.) thanks the Special Postdoctoral Researchers Program of RIKEN.

[1] R. Albert and A.-L. Barabási, Rev. Mod. Phys. **74**, 47 (2002).
[2] S. N. Dorogovtsev and J. F. F. Mendes, Adv. Phys. **51**, 1079 (2002).
[3] M. E. J. Newman, SIAM Rev. **45**, 167 (2003).
[4] R. Albert, H. Jeong, and A.-L. Barabási, Nature (London) **401**, 130 (1999).
[5] M. Faloutsos, P. Faloutsos, and C. Faloutsos, Comput. Commun. **29**, 251 (1999).
[6] F. Liljeros, C. R. Edling, L. A. N. Amaral, H. E. Stanley, and Y. Aberg, Nature (London) **411**, 907 (2001).
[7] R. Pastor-Satorras and A. Vespignani, Phys. Rev. Lett. **86**, 3200 (2001).
[8] M. Boguñá, R. Pastor-Satorras, and A. Vespignani, Phys. Rev. Lett. **90**, 028701 (2003).
[9] R. Pastor-Satorras and A. Vespignani, Phys. Rev. E **65**, 036104 (2002).
[10] Z. Dezsö and A.-L. Barabási, Phys. Rev. E **65**, 055103(R) (2002).
[11] R. Cohen, S. Havlin, and D. ben-Avraham, Phys. Rev. Lett. **91**, 247901 (2003).
[12] M. E. J. Newman, Phys. Rev. Lett. **95**, 108701 (2005).
[13] D. Moore, C. Shannon, and K. Claffy, *Proceedings of the 2nd ACM SIGCOMM Workshop on Internet Measurement* (ACM, New York, NY, 2002), pp. 273–284.
[14] See the malware FAQ on Code Red worm at http://www.sans.org/resources/malwarefaq/code-red.php in the SANS institute.
[15] R. Coico, G. Sunshine, and E. Benjamini, *Immunology: A Short Course* (Wiley, New York, 2003), 5th Ed.
[16] A. Karlen, *Man and Microbes*, 1st ed. (Simon and Schuster, New York, 1996).
[17] C. Castellano and R. Pastor-Satorras, Phys. Rev. Lett. **96**,

038701 (2006).
[18] J. D. Noh and H. Park, Phys. Rev. Lett. **94**, 145702 (2005).
[19] N. Masuda and N. Konno, J. Theor. Biol. (to be published).
[20] M. E. J. Newman, Phys. Rev. Lett. **89**, 208701 (2002).
[21] Y.-Y. Ahn, H. Jeong, and J. D. Noh (unpublished).
[22] D. S. Callaway, J. E. Hopcroft, J. M. Kleinberg, M. E. J. Newman, and S. H. Strogatz, Phys. Rev. E **64**, 041902 (2001); S. N. Dorogovtsev, J. F. F. Mendes, and A. N. Samukhin, *ibid.* **64**, 066110 (2001).
[23] M. Bauer, S. Coulomb, and S. N. Dorogovtsev, Phys. Rev. Lett. **94**, 200602 (2005).
[24] K.-I. Goh, B. Kahng, and D. Kim, Phys. Rev. Lett. **87**, 278701 (2001).